The Rotne-Prager-Yamakawa approximation for periodic systems in a shear flow

Krzysztof A. Mizerski,[1,a)] Eligiusz Wajnryb,[2,a)] Pawel J. Zuk,[3,a)] and Piotr Szymczak[3,a)]
[1]*Department of Magnetism, Institute of Geophysics, Polish Academy of Sciences, Ksiecia Janusza 64, 01-452 Warsaw, Poland*
[2]*Department of Mechanics and Physics of Fluids, Institute of Fundamental and Technological Research, Polish Academy of Sciences, Pawinskiego 5B, 02-106 Warsaw, Poland*
[3]*Institute of Theoretical Physics, Faculty of Physics, University of Warsaw, Hoza 69, 00-681 Warsaw, Poland*

(Received 17 December 2013; accepted 31 March 2014; published online 9 May 2014)

Rotne-Prager-Yamakawa approximation is a commonly used approach to model hydrodynamic interactions between particles suspended in fluid. It takes into account all the long-range contributions to the hydrodynamic tensors, with the corrections decaying at least as fast as the inverse fourth power of the interparticle distances, and results in a positive definite mobility matrix, which is fundamental in Brownian dynamics simulations. In this communication, we show how to construct the Rotne-Prager-Yamakawa approximation for the bulk system under shear flow, which is modeled using the Lees-Edwards boundary conditions. © *2014 AIP Publishing LLC*. [http://dx.doi.org/10.1063/1.4871113]

I. INTRODUCTION

Flow induced phenomena are at the core of soft matter physics – flow drives complex fluids out of equilibrium, changes their internal structure,[1–3] unfolds proteins and DNA,[4,5] accelerates the aggregation processes,[6,7] induces polymer migration in capillaries[8] and phase separation in complex fluids.[9,10] Most of these phenomena are already observed for a simple, linear shear flow, such as that which occurs in a Couette device. In fact a nonzero shear component appears whenever a fluid flows along a surface, including different kinds of capillary flows, hence the shear-induced effects are indeed ubiquitous in soft matter systems.

Another important aspect of the dynamics of suspended particles is the presence of hydrodynamic interactions (HI): the particles excite long-ranged flows as they move, which then influence all other particles in the system and modify the ambient fluid velocity field. The HI were shown to play a key role in variety of processes: they affect the values of diffusion coefficients in colloidal suspensions,[11] change the kinetic pathways of phase separation in binary mixtures,[12] alter the kinetics of macromolecule adsorption on surfaces,[13] affect the characteristics of the coil-stretch transition in polymers,[14] the timescales of protein folding and unfolding[15,16] and the dynamics of lipid membranes self assembly.[17] The inclusion of HI is thus essential for a proper modeling of the dynamics of complex fluids and biopolymers, both with and without the flow.

In general, there are two ways in which the uniform shear can be introduced in the molecular dynamics simulations. The first is to confine the system between two parallel plates and translate one plate parallel to another at a constant speed. The disadvantage of such a setup is the presence of strong wall effects, which are undesirable, unless our intention is to model the flow in nanochannels. Alternatively, to mitigate wall effects and more effectively simulate the bulk, one uses the periodic cell of the Lees-Edwards kind,[18,19] which deforms, becoming progressively more titled with time (cf. Fig. 1). For a simple shear of a form $\dot{\gamma} z \mathbf{e}_x$ the tilting angle (i.e., the angle between the instantaneous direction of the tilted z axis and its original direction) varies with the shear rate $\dot{\gamma}$ and time t as[19]

$$\theta = \arctan\left(\frac{\dot{\gamma} L_z t \bmod L_x}{L_z}\right), \tag{1}$$

where mod stands for the modulo operation. The use of Lees-Edwards cell allows the simulation of a bulk material under shear, however the inclusion of HI in this case is far from trivial, with the details strongly depending on a particular model used to represent the hydrodynamic interactions, see, e.g., Ref. 20 for an implementation of the Lees-Edwards boundary conditions for smoothed particle hydrodynamics; Ref. 21 for a similar derivation for the lattice Boltzmann method; and Ref. 22 for multi-particle collision dynamics. In this paper, we show how to include hydrodynamic interactions in the deformed Lees-Edwards cell using the Rotne-Prager-Yamakawa (RPY) approximation for the hydrodynamic tensors. This approximation is based on the following idea: when a force (or torque) is applied to particle i, that particle begins to move, inducing flow in the bulk of the fluid. The extent to which this additional flow affects translational and rotational velocities of another particle (j) is then calculated using Faxen's laws.[23] In that way one neglects not only the multi-body effects (involving three and more particles) but also the higher-order terms in two-particle interactions (e.g., the impact of the movement of particle j back on particle i). The Rotne-Prager-Yamakawa tensor is by far the most popular method of accounting for HI in soft matter modeling.[24] The RPY is a far-field approximation: it incorporates all the long-ranged contributions to the hydrodynamic tensors, with the corrections decaying at least as fast as the inverse fourth power of the interparticle distances, but is less accurate at smaller

a)Electronic addresses: kamiz@igf.edu.pl; piotr.szymczak@fuw.edu.pl; ewajnryb@ippt.gov.pl; and pawel.zuk@fuw.edu.pl

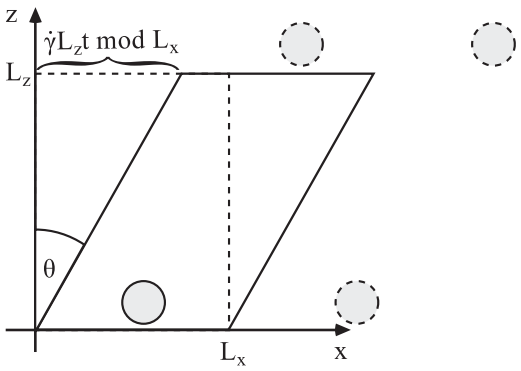

FIG. 1. Lees-Edwards boundary conditions for a simple shear flow: as time advances the simulation cell is deformed with the shear flow such that the shearing boundaries always align with the image cells. The initial cell is depicted with the dashed line. Whenever the simulation cell deforms by $\arctan L_x/L_z$ it is reset to prevent it from deforming indefinitely in one direction.

distances. In particular, when the particles overlap, the hydrodynamic tensors calculated based on RPY may become non-positive definite, which causes a problem in the Brownian dynamics simulations, where the square root of mobility matrix is needed. To avoid this problem, one usually uses a regularizing correction for the overlapping particles, which is not singular at $R_{ij} = 0$ and positive definite for all the particle configurations. In a recent paper[25] we have re-derived the original RPY tensor using direct integration of force densities over the sphere surfaces and used this approach to derive the regularizing corrections for rotational and dipolar components of the generalized mobility matrix. We have also shown how to generalize the RPY approach to different-sized particles.[26] Here, this formalism will be used to derive the explicit form of hydrodynamic matrices in the periodic system under the shear.

II. THE ROTNE-PRAGER-YAMAKAWA APPROXIMATION

We consider a suspension of N identical spherical particles of different radii a_i, in an incompressible fluid of viscosity η at a low Reynolds number. The particles are immersed in a linear shear flow

$$\mathbf{v}_\infty(\mathbf{r}) = \mathbf{K}_\infty \cdot \mathbf{r}, \tag{2}$$

where $\mathbf{K}_\infty$ is the constant velocity gradient matrix, e.g., for a simple shear flow

$$\mathbf{K}_\infty = \begin{bmatrix} 0 & 0 & \dot{\gamma} \\ 0 & 0 & 0 \\ 0 & 0 & 0 \end{bmatrix}, \quad \dot{\gamma} = \text{const}. \tag{3}$$

Due to the linearity of the Stokes equations, the forces and torques exerted by the fluid on the particles ($\boldsymbol{\mathcal{F}}_j$ and $\boldsymbol{\mathcal{T}}_j$) depend linearly on translational and rotational velocities of the particles ($\mathbf{U}_i$, $\boldsymbol{\Omega}_i$). This relation defines the generalized friction matrix $\boldsymbol{\zeta}$

$$\begin{pmatrix} \boldsymbol{\mathcal{F}}_j \\ \boldsymbol{\mathcal{T}}_j \end{pmatrix} = -\sum_i \begin{pmatrix} \boldsymbol{\zeta}_{ji}^{tt} & \boldsymbol{\zeta}_{ji}^{tr} & \boldsymbol{\zeta}_{ji}^{td} \\ \boldsymbol{\zeta}_{ji}^{rt} & \boldsymbol{\zeta}_{ji}^{rr} & \boldsymbol{\zeta}_{ji}^{rd} \end{pmatrix} \cdot \begin{pmatrix} \mathbf{v}_\infty(\mathbf{R}_i) - \mathbf{U}_i \\ \boldsymbol{\omega}_\infty(\mathbf{R}_i) - \boldsymbol{\Omega}_i \\ \mathbf{E}_\infty \end{pmatrix}, \tag{4}$$

where $\boldsymbol{\zeta}^{pq}$ (with $p = t, r$ and $q = t, r, d$) are the Cartesian tensors and the superscripts t, r, and d correspond to the translational, rotational, and dipolar components, respectively. The tensor $\mathbf{E}_\infty$ is the symmetric part of $\mathbf{K}_\infty$ in (3) and $\boldsymbol{\omega}_\infty = \frac{1}{2}\nabla \times \mathbf{v}_\infty(\mathbf{R}_i) = \frac{1}{2}\boldsymbol{\epsilon} : \mathbf{K}_\infty$ is the vorticity of the incident flow. Finally, $\mathbf{R}_i$ corresponds to the position of particle i. The reciprocal relation giving velocities of particles moving under external forces/torques in external flow $\mathbf{v}_\infty$ is determined by generalized mobility matrix $\boldsymbol{\mu}$ is given by[11]

$$\begin{pmatrix} \mathbf{U}_i \\ \boldsymbol{\Omega}_i \end{pmatrix} = \begin{pmatrix} \mathbf{v}_\infty(\mathbf{R}_i) \\ \boldsymbol{\omega}_\infty(\mathbf{R}_i) \end{pmatrix} + \sum_j \left[\begin{pmatrix} \boldsymbol{\mu}_{ij}^{tt} & \boldsymbol{\mu}_{ij}^{tr} \\ \boldsymbol{\mu}_{ij}^{rt} & \boldsymbol{\mu}_{ij}^{rr} \end{pmatrix} \cdot \begin{pmatrix} \boldsymbol{\mathcal{F}}_j \\ \boldsymbol{\mathcal{T}}_j \end{pmatrix} \right] + \begin{pmatrix} \mathbf{C}_i^t \\ \mathbf{C}_i^r \end{pmatrix} : \mathbf{E}_\infty, \tag{5}$$

where the shear disturbance tensor $\mathbf{C}$ elements are defined as

$$\mathbf{C}_i^t = \sum_j \boldsymbol{\mu}_{ij}^{td}, \quad \mathbf{C}_i^r = \sum_j \boldsymbol{\mu}_{ij}^{rd}. \tag{6}$$

In the case of single-particle the mobility matrixes reduce to

$$\boldsymbol{\mu}_{ii}^{tt} = \frac{1}{\zeta^{tt}}\mathbf{1}, \quad \boldsymbol{\mu}_{ii}^{rr} = \frac{1}{\zeta^{rr}}\mathbf{1}, \quad \boldsymbol{\mu}_{ii}^{tr} = \boldsymbol{\mu}_{ii}^{rt} = 0, \tag{7}$$

with the friction coefficients for a spherical particle given by $\zeta^{tt} = 6\pi\eta a$ and $\zeta^{rr} = 8\pi\eta a^3$.

In Ref. 25 we have shown that within the Rotne-Prager-Yamakawa formalism the mobility tensors can be expressed as

$$\boldsymbol{\mu}_{ij}^{tt} = \langle \mathbf{w}_i^t | \mathbf{T}_\mathrm{H} | \mathbf{w}_j^t \rangle, \quad \boldsymbol{\mu}_{ij}^{rr} = \langle \mathbf{w}_i^r | \mathbf{T}_\mathrm{H} | \mathbf{w}_j^r \rangle, \tag{8a}$$

$$\boldsymbol{\mu}_{ij}^{rt} = \langle \mathbf{w}_i^r | \mathbf{T}_\mathrm{H} | \mathbf{w}_j^t \rangle, \quad \boldsymbol{\mu}_{ij}^{tr} = \langle \mathbf{w}_i^t | \mathbf{T}_\mathrm{H} | \mathbf{w}_j^r \rangle, \tag{8b}$$

$$\boldsymbol{\mu}_{ij}^{td} : \mathbf{E}_\infty = \langle \mathbf{w}_i^t | \mathbf{T}_\mathrm{H} | \mathbf{w}_j^c \rangle : \mathbf{E}_\infty, \tag{8c}$$

$$\boldsymbol{\mu}_{ij}^{rd} : \mathbf{E}_\infty = \langle \mathbf{w}_i^r | \mathbf{T}_\mathrm{H} | \mathbf{w}_j^c \rangle : \mathbf{E}_\infty, \tag{8d}$$

where we use the bra-ket notation defined in the following way

$$\boldsymbol{\mu}_{ij}^{pq} = \langle \mathbf{w}_i^p | \mathbf{T}_\mathrm{H} | \mathbf{w}_j^q \rangle = \int \mathrm{d}\mathbf{r}' \int \mathrm{d}\mathbf{r}'' \left[\mathbf{w}_i^p(\mathbf{r}') \right]^T \cdot \mathbf{T}_\mathrm{H}(\mathbf{r}' - \mathbf{r}'') \cdot \mathbf{w}_j^q(\mathbf{r}''), \tag{9}$$

with $p, q = r, t$ and in an analogous way for the dipolar component. In the above the upper index T denotes the tensor transposition and $\mathbf{T}_\mathbf{H}(\mathbf{r}' - \mathbf{r}'')$ is the Green's function for the Stokes flow, which for a periodic system is given by the Hasimoto tensor[27] (see below). Next, the tensors $\mathbf{w}^p(\mathbf{r})$ are defined in the following way

$$\mathbf{w}_i^t(\mathbf{r}) = \frac{1}{4\pi a^2}\mathbf{1}\delta(\rho_i - a_i), \tag{10a}$$

$$\mathbf{w}_i^r(\mathbf{r}) = \frac{3}{8\pi a^3}\boldsymbol{\epsilon}\cdot\hat{\boldsymbol{\rho}}_i\delta(\rho_i - a_i), \tag{10b}$$

$$\mathbf{w}^c(\mathbf{r}) : \mathbf{E}_\infty = 3\eta\delta(\rho_i - a_i)\mathbf{E}_\infty\cdot\hat{\boldsymbol{\rho}}_i, \tag{10c}$$

where $(\boldsymbol{\epsilon}\cdot\hat{\boldsymbol{\rho}}_i)_{\alpha\beta} = \epsilon_{\alpha\beta\gamma}\hat{\rho}_{i\gamma}$, $\epsilon_{\alpha\beta\gamma}$ is the Levi-Civita symbol, and $\boldsymbol{\rho}_i = \mathbf{r} - \mathbf{R}_i$. The first of the above tensors multiplied by force, $\mathbf{w}^t\cdot\boldsymbol{\mathcal{F}}$, corresponds to the force density on the surface of a sphere due to the force $\boldsymbol{\mathcal{F}}$ acting on that sphere. Similarly, $\mathbf{w}^r\cdot\boldsymbol{\mathcal{T}}$ gives the contribution to the force density due to the torque $\boldsymbol{\mathcal{T}}$. Finally, the product $\mathbf{w}^c(\mathbf{r}) : \mathbf{E}_\infty$ corresponds to the surface force density due to the straining fluid motion $\mathbf{E}_\infty\cdot\mathbf{r}$.

Note that since in the evolution equations (5) the mobility components $\boldsymbol{\mu}_{ij}^{td}$ and $\boldsymbol{\mu}_{ij}^{rd}$ appear only in the form of a double-dot product with a symmetric and traceless tensor $\mathbf{E}_\infty$, there is a certain freedom of choice of the final form of those matrices, namely, addition of an antisymmetric tensor or a trace does not alter the final equations. We will choose the simplest form, desirable from the point of view of numerical modeling of suspension dynamics.

The hydrodynamic tensors defined above can then be used in the Brownian dynamics scheme describing the evolution of the position vector $\mathbf{R}_i$ and the direction vector $\hat{\mathbf{e}}_i$ (e.g., the magnetic dipole moment) of each particle $i = 1, \ldots, N$:[28]

$$\mathbf{R}_i(t+\Delta t) = \mathbf{R}_i(t) + \mathbf{U}_i^C\Delta t + \sum_j \boldsymbol{\mu}_{ij}^{tt}\cdot\boldsymbol{\mathcal{F}}_j\Delta t + \sum_j \boldsymbol{\mu}_{ij}^{tr}\cdot\boldsymbol{\mathcal{T}}_j\Delta t + \boldsymbol{\Gamma}_i^t, \tag{11}$$

$$\hat{\mathbf{e}}_i(t+\Delta t) = \hat{\mathbf{e}}_i(t) + \left[\boldsymbol{\Omega}_i^C\,\Delta t + \sum_j \boldsymbol{\mu}_{ij}^{rt}\cdot\boldsymbol{\mathcal{F}}_j\Delta t + \sum_j \boldsymbol{\mu}_{ij}^{rr}\cdot\boldsymbol{\mathcal{T}}_j\Delta t + \boldsymbol{\Gamma}_i^r\right]\times\hat{\mathbf{e}}_i(t), \tag{12}$$

where

$$\mathbf{U}_i^C = \mathbf{K}_\infty\cdot\mathbf{R}_i(t) + \mathbf{C}_i^t : \mathbf{E}_\infty, \tag{13}$$

$$\boldsymbol{\Omega}_i^C = \frac{1}{2}\nabla\times(\mathbf{K}_\infty\cdot\mathbf{R}_i) + \mathbf{C}_i^r : \mathbf{E}_\infty = \frac{1}{2}\boldsymbol{\epsilon} : \mathbf{K}_\infty + \mathbf{C}_i^r : \mathbf{E}_\infty. \tag{14}$$

The stochastic displacement $\boldsymbol{\Gamma}$ is a Gaussian random variable with zero mean and the covariance

$$\langle\boldsymbol{\Gamma}(\Delta t)\boldsymbol{\Gamma}(\Delta t)\rangle = 2k_BT\boldsymbol{\mu}\,\Delta t, \tag{15}$$

$$k_BT\boldsymbol{\mu} = \boldsymbol{\mathcal{E}}\cdot\boldsymbol{\mathcal{E}}^T, \quad \langle g_i g_j\rangle = \delta_{ij}, \quad \boldsymbol{\Gamma}(\Delta t) = \sqrt{2\,\Delta t}\,\boldsymbol{\mathcal{E}}\cdot\mathbf{g}, \tag{16}$$

where the $6N\times 6N$ matrix $\boldsymbol{\mu}$ comprising $\boldsymbol{\mu}^{tt}$, $\boldsymbol{\mu}^{tr}$, $\boldsymbol{\mu}^{rt}$ and $\boldsymbol{\mu}^{rr}$ is called the N-particle mobility matrix and $\mathbf{g}$ denotes a vector of $6N$ independent, normalized Gaussian processes. In the above we have neglected the terms involving divergence of mobility tensors (cf. Ref. 28), since they vanish within the RPY approximation. However, when one goes beyond RPY approximation and includes many-body effects in hydrodynamic interactions, the divergence of mobility matrix becomes non-zero and needs to be taken into account in Brownian dynamics simulation schemes.[29]

III. THE HASIMOTO TENSOR

The Hasimoto tensor can be conveniently expressed as[30]

$$\mathbf{T}_\mathrm{H}(\mathbf{r}) = \frac{1}{4\pi\eta}(S_1(\mathbf{r})\mathbf{1} - \nabla\nabla S_2(\mathbf{r})), \tag{17}$$

where the two scalar functions S_1 and S_2 have the periodicity of the lattice and satisfy

$$S_1(\mathbf{r}) = \sum_\mathbf{n} r_\mathbf{n}^{-1}\mathrm{erfc}\left(\frac{r_\mathbf{n}}{\sqrt{2\sigma^2}}\right) + \frac{4\pi}{V}\sum_\mathbf{n}{}' \frac{1}{k_\mathbf{n}^2}\mathrm{e}^{-k_\mathbf{n}^2\sigma^2/2}\cos(\mathbf{k}_\mathbf{n}\cdot\mathbf{r}) - \frac{2\sigma^2\pi}{V}, \tag{18}$$

$$S_2(\mathbf{r}) = \frac{1}{2\sqrt{\pi}}\sum_\mathbf{n}\left[\sqrt{\pi}r_\mathbf{n}\mathrm{erfc}\left(\frac{r_\mathbf{n}}{\sqrt{2\sigma^2}}\right) - \sqrt{2\sigma^2}\mathrm{e}^{-r_\mathbf{n}^2/2\sigma^2}\right] - \frac{4\pi}{V}\sum_\mathbf{n}{}'\left(1+\frac{1}{2}\sigma^2k_\mathbf{n}^2\right)\frac{1}{k_\mathbf{n}^4}\mathrm{e}^{-k_\mathbf{n}^2\sigma^2/2} \times\cos(\mathbf{k}_\mathbf{n}\cdot\mathbf{r}) + \frac{\sigma^4\pi}{2V}, \tag{19}$$

where σ is a splitting parameter for the Ewald summations, whereas $\mathbf{n} = [n_1, n_2, n_3]$ is a vector of integers numbering the cells in the real lattice,

$$\mathbf{r}_\mathbf{n} = \mathbf{r} + \mathbf{L}\cdot\mathbf{n}, \tag{20}$$

or in the reciprocal lattice,

$$\mathbf{k}_\mathbf{n} = 2\pi\mathbf{n}\cdot\mathbf{L}^{-1}. \tag{21}$$

The prime at the summation symbol in (19) indicates that the term $\mathbf{n} = 0$ is to be omitted. In the above $\mathbf{L}\cdot\mathbf{n}$ is the lattice displacement between the particle and its periodic images and $\mathbf{L}$ is the lattice matrix the columns of which are the lattice vectors. Next, the volume of the elementary cell $V = \det\mathbf{L}$. In a simulation, the implementation of the Lees-Edwards boundary conditions requires that the lattice matrix depends on time, as given by Eq. (1). In the case at hand, for the coordinate axes defined as in (3), the lattice matrix takes the following form

$$\mathbf{L} = \begin{bmatrix} L_x & 0 & \dot{\gamma}L_zt \bmod L_x \\ 0 & L_y & 0 \\ 0 & 0 & L_z \end{bmatrix}, \tag{22}$$

where L_x, L_y, and L_z determine the initial size of the cell.

In practice, the summations (18) and (19) are evaluated including only the terms larger than a certain small value, i.e., satisfying the inequality

$$\exp\left[-\frac{r_\mathbf{n}^2}{2\sigma^2}\right] \geq \epsilon, \tag{23}$$

in the real sum and

$$\exp\left[-\frac{k_\mathbf{n}^2\sigma^2}{2}\right] \geq \epsilon, \tag{24}$$

in the reciprocal sum. Using (20) and (21), asymptotically (for large $|\mathbf{n}|$) this can be reduced to the following conditions for vectors $\mathbf{n}$,

$$\mathbf{n}\cdot\mathbf{N}_\mathrm{R}\cdot\mathbf{n} \leq 1, \tag{25}$$

$$\mathbf{n}\cdot\mathbf{N}_{\mathrm{F}}\cdot\mathbf{n}\le 1, \tag{26}$$

where

$$\mathbf{N}_{\mathrm{R}}=\frac{1}{2\sigma^2\ln\epsilon^{-1}}(\mathbf{L}^{\mathrm{T}}\cdot\mathbf{L}), \tag{27}$$

and

$$\mathbf{N}_{\mathrm{F}}=\frac{(2\pi)^2\sigma^2}{2\ln\epsilon^{-1}}(\mathbf{L}^{\mathrm{T}}\cdot\mathbf{L})^{-1}. \tag{28}$$

Equations (25) and (26) define the interiors of the ellipsoids in (n_x, n_y, n_z) space. Note that in the case of strongly skewed periodic cells the corresponding ellipsoids are highly elongated.

The number of terms satisfying the conditions (25) and (26) (and thus the numerical cost) are measured by the volumes of these ellipsoids,

$$V_{\mathrm{R}}=\frac{1}{\det\mathbf{N}_{\mathrm{R}}}=(2\sigma^2\ln\epsilon^{-1})^3V^{-2}, \tag{29}$$

$$V_{\mathrm{F}}=\frac{1}{\det\mathbf{N}_{\mathrm{F}}}=\left(\frac{2\ln\epsilon^{-1}}{(2\pi)^2\sigma^2}\right)^3V^2, \tag{30}$$

The optimal σ which minimizes $V_{\mathrm{R}}+V_{\mathrm{F}}$ is evaluated from the condition $V_{\mathrm{R}}=V_{\mathrm{F}}$ and is given by

$$\sigma=\frac{V^{1/3}}{\sqrt{2\pi}}, \tag{31}$$

independent of ϵ.

The two scalar functions $S_1(\mathbf{r})$ and $S_2(\mathbf{r})$ in (17) satisfy $\nabla^2S_2=S_1$. However, direct computation of $\nabla^2S_2-S_1$ leads to a sum of non-zero terms both in the real and reciprocal spaces. This sum vanishes because of the well-known Parseval's equality.[31] Therefore it is important to keep in mind that if, e.g., ∇^2S_2 were used in the expression for the Hasimoto tensor (17) instead of S_1, the final formulae for the mobility, although correct, would be given in a far more complicated form, possessing a number of terms that could be gathered to sum up to zero. In this paper we try to present all the formulae in the simplest way possible, making use of the Parseval's equality to remove terms that sum up to zero. In particular the *tt* component of the mobility matrix for periodic systems has been obtained before in a quite complicated form by Beenakker (1986)[32] and modified to account for bead overlaps by Jain *et al.* (2012).[33] Stoltz *et al.* (2006)[34] have considered the external shear flow and the Lees-Edwards boundary conditions, however, just like Beenakker (1986)[32] and Jain *et al.* (2012)[33] they studied only the translational degrees of freedom and did not consider the effect of hydrodynamic interactions on the flow, i.e., the $\boldsymbol{\mu}^{td}$ component of the mobility. Monodisperse systems (with equal particle radii) with external shear were also studied by Brady *et al.* (1988),[35] but without deriving the regularizing corrections for particle overlaps; moreover, they have not provided the explicit formulae for all the mobility matrix components. The same regularizing correction for overlaps as derived below has been used by Zhou and Chen (2006),[36] but, again only in the case of translational degrees of freedom and in absence of external shear. Here we present all the translational-rotational-dipolar components of the mobility matrix, (see Appendix A for the explicit formulae with the corrections for overlaps given in Appendix B), and moreover, the final formulae are given in a compact and attractive (simple) form from the point of view of numerical computations.

IV. THE HYDRODYNAMIC MATRICES

The mobility matrix, including the additional corrections for overlapping particles can be cast in the following form:

$$\boldsymbol{\mu}^{tt}_{ij}(\mathbf{R}_{ij};a_{i,},a_j)=\left[\frac{1}{\zeta^{tt}}\mathbf{1}+\mathbf{M}^{tt}_S(a_i)\right]\delta_{ij}+[\mathbf{M}^{tt}(\mathbf{R}_{ij};a_{i,},a_j)+\mathbf{Y}^{tt}(\widetilde{\mathbf{R}}_{ij};a_i,a_j)](1-\delta_{ij}), \tag{32}$$

$$\boldsymbol{\mu}^{rr}_{ij}(\mathbf{R}_{ij};a_{i,},a_j)=\left[\frac{1}{\zeta^{rr}}\mathbf{1}+\mathbf{M}^{rr}_S\right]\delta_{ij}+[\mathbf{M}^{rr}(\mathbf{R}_{ij})+\mathbf{Y}^{rr}(\widetilde{\mathbf{R}}_{ij};a_{i,},a_j)](1-\delta_{ij}), \tag{33}$$

$$\boldsymbol{\mu}^{rt}_{ij}(\mathbf{R}_{ij};a_{i,},a_j)=\mathbf{M}^{rt}_S\delta_{ij}+[\mathbf{M}^{rt}(\mathbf{R}_{ij})+\mathbf{Y}^{rt}(\widetilde{\mathbf{R}}_{ij};a_{i,},a_j)](1-\delta_{ij}), \tag{34}$$

$$\boldsymbol{\mu}^{tr}_{ij}(\mathbf{R}_{ij};a_{i,},a_j)=\boldsymbol{\mu}^{rt}_{ij}(\mathbf{R}_{ij};a_{j,},a_i), \tag{35}$$

$$\boldsymbol{\mu}^{td}_{ij}(\mathbf{R}_{ij};a_{i,},a_j)=\mathbf{M}^{td}_S(a_i)\delta_{ij}+[\mathbf{M}^{td}(\mathbf{R}_{ij};a_{i,},a_j)+\mathbf{Y}^{td}(\widetilde{\mathbf{R}}_{ij};a_{i,},a_j)](1-\delta_{ij}), \tag{36}$$

$$\boldsymbol{\mu}^{rd}_{ij}(\mathbf{R}_{ij};a_{i,},a_j)=\mathbf{M}^{rd}_S(a_i)\delta_{ij}+[\mathbf{M}^{rd}(\mathbf{R}_{ij};a_j)+\mathbf{Y}^{rd}(\widetilde{\mathbf{R}}_{ij};a_{i,},a_j)](1-\delta_{ij}), \tag{37}$$

where $\widetilde{\mathbf{R}}_{ij}$ is the vector connecting particle i with the nearest periodic image of particle j and the hydrodynamic interactions with the particle's own periodic images are included through the following functions (self-interaction terms):

$$\mathbf{M}^{tt}_S(a)=\lim_{r\to0}\left(\mathbf{1}+\frac{a^2}{3}\nabla^2\right)[\mathbf{T}_{\mathrm{H}}(\mathbf{r})-\mathbf{T}_0(\mathbf{r})], \tag{38}$$

$$\mathbf{M}^{rr}_S=-\frac{1}{4}\lim_{r\to0}\nabla^2[\mathbf{T}_{\mathrm{H}}(\mathbf{r})-\mathbf{T}_0(\mathbf{r})], \tag{39}$$

$$\mathbf{M}^{rt}_S=\frac{1}{2}\lim_{r\to0}\nabla\times[\mathbf{T}_{\mathrm{H}}-\mathbf{T}_0(\mathbf{r})]=0, \tag{40}$$

$$\mathbf{M}^{td}_S(a):\mathbf{E}_\infty=\frac{20}{3}\pi\eta a^3\lim_{r\to0}\left\{\left[\left(1+\frac{4a^2}{15}\nabla^2\right)\times(\mathbf{T}_{\mathrm{H}}(\mathbf{r})-\mathbf{T}_0(\mathbf{r}))\right]\overleftarrow{\nabla}\right\}:\mathbf{E}_\infty=0, \tag{41}$$

$$\mathbf{M}^{rd}_S(a):\mathbf{E}_\infty=\frac{10}{3}\pi\eta a^3\lim_{r\to0}\{[\nabla\times(\mathbf{T}_{\mathrm{H}}(\mathbf{r})-\mathbf{T}_0(\mathbf{r}))]\overleftarrow{\nabla}\}:\mathbf{E}_\infty, \tag{42}$$

with $a=a_i=a_j$, since $\mathbf{M}_S$ is multiplied by δ_{ij} in (32)–(37). Next, $\mathbf{T}_0(\mathbf{r})$ is the Oseen tensor:[23]

$$\mathbf{T}_0(\mathbf{r})=\frac{1}{8\pi\eta r}(\mathbf{1}+\hat{\mathbf{r}}\hat{\mathbf{r}}). \tag{43}$$

Note that $\mathbf{M}_S^{rr}$ and $\mathbf{M}_S^{rt}$ do not depend on a_i but only on the lattice characteristics. The interactions with other particles and their periodic images are described by

$$\mathbf{M}^{tt}(\mathbf{R}_{ij};a_{i,},a_j)=\left(\mathbf{1}+\frac{A_{ij}^2}{3}\nabla^2\right)\mathbf{T}_{\mathrm{H}}(\mathbf{R}_{ij}),\tag{44}$$

$$\mathbf{M}^{rr}(\mathbf{R}_{ij})=-\frac{1}{4}\nabla^2\mathbf{T}_{\mathrm{H}}(\mathbf{R}_{ij}),\tag{45}$$

$$\mathbf{M}^{rt}(\mathbf{R}_{ij})=\frac{1}{2}\nabla\times\mathbf{T}_{\mathrm{H}}(\mathbf{R}_{ij}),\tag{46}$$

$$\mathbf{M}^{td}(\mathbf{R}_{ij};a_{i,},a_j):\mathbf{E}_\infty=\frac{20}{3}\pi\eta a_j^3\left\{\left[\left(1+\frac{4\mathscr{A}_{ij}^2}{15}\nabla^2\right)\mathbf{T}_{\mathrm{H}}(\mathbf{R}_{ij})\right]\overleftarrow{\nabla}\right\}:\mathbf{E}_\infty,\tag{47}$$

$$\mathbf{M}^{rd}(\mathbf{R}_{ij};a_j):\mathbf{E}_\infty=\frac{10}{3}\pi\eta a_j^3\{[\nabla\times\mathbf{T}_{\mathrm{H}}(\mathbf{R}_{ij})]\overleftarrow{\nabla}\}:\mathbf{E}_\infty.\tag{48}$$

In the above,

$$A_{ij}^2=\frac{a_i^2+a_j^2}{2},\quad \mathscr{A}_{ij}^2=\frac{5a_i^2+3a_j^2}{8},\tag{49}$$

where ∇ is a differential operator with respect to $\mathbf{R}_{ij}$ and $[\mathbf{T}_{\mathrm{H}}(\mathbf{R}_{ij})\overleftarrow{\nabla}]_{\alpha\beta\gamma}=\partial_\gamma T_{\mathrm{H}\alpha\beta}(\mathbf{R}_{ij})$. Note that here $\mathbf{M}^{rr}(\mathbf{R}_{ij})$ and $\mathbf{M}^{rt}(\mathbf{R}_{ij})$ do not depend neither on a_i nor on a_j, whereas $\mathbf{M}^{rd}(\mathbf{R}_{ij};a_j)$ does not depend on a_i. The regularizing corrections $\mathbf{Y}^{tt}(\widetilde{\mathbf{R}}_{ij};a_{i,},a_j)$, $\mathbf{Y}^{rr}(\widetilde{\mathbf{R}}_{ij};a_{i,},a_j)$, $\mathbf{Y}^{rt}(\widetilde{\mathbf{R}}_{ij};a_{i,},a_j)$, $\mathbf{Y}^{td}(\widetilde{\mathbf{R}}_{ij};a_{i,},a_j)$, and $\mathbf{Y}^{rd}(\widetilde{\mathbf{R}}_{ij};a_i,a_j)$ are non-zero only in the cases of overlap between the particles. They were derived with the use of the method presented in Ref. 25 (for a detailed explanation of steps leading to the final formulae see the supplementary material of Ref. 25). For example, the translational-translational correction can be written as

$$\mathbf{Y}^{tt}(\mathbf{R}_{ij};a_{i,},a_j)=\langle\mathbf{w}_i^t|\mathbf{T}_0(\mathbf{R}_{ij})|\mathbf{w}_j^t\rangle-\mathbf{D}^t(\mathbf{R}_{ij},a_i)\mathbf{D}^t(\mathbf{R}_{ij},a_j)\mathbf{T}_0(\mathbf{R}_{ij}),\tag{50}$$

where $\mathbf{D}^t(\mathbf{R};a_i)$ is the differential operator defined by

$$\mathbf{D}^t(\mathbf{R};a_i)=\mathbf{1}\left(1+\frac{a_i^2}{6}\nabla_{\mathbf{R}}^2\right).\tag{51}$$

These corrections were shown to be independent of the form of the Green's function for the particular geometry considered.[25]

The complete set of explicit formulae for the regularizing corrections for different-sized spheres, which can be derived based on considerations presented in Ref. 26, is provided in Appendix B. The final formulae for the hydrodynamic matrices for nonoverlapping spheres are given in Appendix A.

It is of interest to point out that the representation chosen in (32)–(37) for each matrix is, in fact, equivalent to

$$\boldsymbol{\mu}_{ij}^{pq}(\mathbf{R}_{ij};a_{i,},a_j)=\mathbf{M}^{pq}(\mathbf{R}_{ij};a_{i,},a_j)+\mathbf{Y}^{pq}(\widetilde{\mathbf{R}}_{ij};a_{i,},a_j),\tag{52}$$

which results from the fact that the full self term is obtained as a limit of $\mathbf{M}^{pq}$ and $\mathbf{Y}^{pq}$, with $p, q = t, r, d$ when R_{ij} tends to zero and $a_i = a_j = a$, i.e., $\lim_{R_{ij}\to 0}\mathbf{M}^{pq}(\mathbf{R}_{ij};a,a) = \mathbf{M}_S^{pq}(a)$ for any p and q, $\lim_{R_{ij}\to 0}\mathbf{Y}^{tt}(\widetilde{\mathbf{R}}_{ij};a,a)=\mathbf{1}/\zeta^{tt}$, $\lim_{R_{ij}\to 0}\mathbf{Y}^{rr}(\widetilde{\mathbf{R}}_{ij};a,a)=\mathbf{1}/\zeta^{rr}$, and $\lim_{R_{ij}\to 0}\mathbf{Y}^{pq}(\widetilde{\mathbf{R}}_{ij};a,a)=0$ for $(p,q)=(r,t),(t,r),(t,d),(r,d)$. Although this representation is more compact, the second representation, with the full self term explicitly written down is more useful from the technical point of view.

This completes our derivation making all the terms in the Brownian dynamics scheme (11)-(12) directly computable, thus allowing for simulations of time evolution of periodic systems with external shear under the Rotne-Prager-Yamakawa approximation.

V. ILLUSTRATIVE EXAMPLE

To illustrate the accuracy of RPY approximation we will compare it with virtually exact multipole series expansion method (MLTP). The setup consists of two rigidly connected particles (dumbbell) of the same radius a inside a cuboid of dimensions $24a \times 4a \times 4a$ in periodic boundary conditions. Both spheres lie on the x axis with the distance between their centers, R_{12}, in the range $(0, 10a)$. Fig. 2 shows the friction coefficient of such a dumbbell $\zeta_\parallel = \zeta_{xx}^{tt}$ and $\zeta_\perp = \zeta_{tt}^{yy} = \zeta_{tt}^{zz}$ as a function of R_{12}. The discrepancy between both methods is negligible up to about $R_{12} = 3a$. For smaller distances the curves start to diverge with a relative error up to

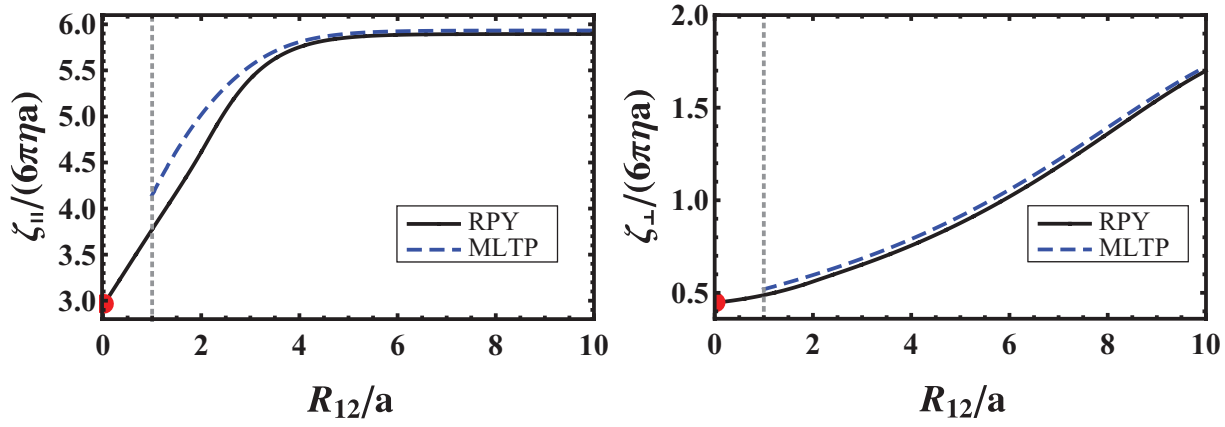

FIG. 2. Friction coefficient of the dumbbell parallel ($\zeta_\parallel$) and perpendicular ($\zeta_\perp$) to its axis as a function of the distance between the spheres, R_{12}.

10% at $R_{12} = a$. Note that the multipole results are plotted down to $R_{12} = a$ only. As noted in Ref. 26 this is due to a fundamental property of the displacement theorem,[37] by means of which one expands the singular flows generated by one sphere into regular flows about the centre of another sphere in the multipole method. Namely, when the two spheres are so close that the centre of the smaller one gets inside the larger one, the aforementioned expansion ceases to be convergent. Even though one cannot use the displacement theorem to calculate the friction for $R_{12} < a$, one can still get the limiting result $\lim_{R_{12}\to 0} \boldsymbol{\zeta}$, as it corresponds simply to a single-particle friction matrix in a periodic lattice. The corresponding points are marked by red dots in Fig. 2. For the particular lattice geometry considered here these limiting results differ by less than 0.5% from the predictions of RPY approximation (solid line in Fig. 2), although this error would increase as the ratio of the particle radius to the box size increases.

VI. CONCLUDING REMARKS

In this paper we have provided explicitly the full set of equations and formulae for modeling the dynamics of periodic suspensions of spherical particles with different radii in external shear flow within the Rotne-Prager-Yamakawa approximation. Care has been taken to provide the final formulae in a simple algebraic form, i.e., to remove terms which can be summed up to zero due to the Parseval's equality. The regularizing corrections for both $\boldsymbol{\mu}$ and $\mathbf{C}$ for the case of overlaps between particles are also provided. The way that hydrodynamic matrices are constructed ensures the positive definiteness of the mobility matrix $\boldsymbol{\mu}$ and both $\boldsymbol{\mu}$ and $\mathbf{C}$ are devoid of singularities, no matter the relative positions of particles.

The obtained formulae allow for efficient numerical calculation of bulk properties and dynamics of soft matter systems in the external shear flow.

ACKNOWLEDGMENTS

K.A.M. and E.W. acknowledge the support of the Polish National Science Centre (Grant No. 2012/05/B/ST8/03010). P.J.Z. acknowledges the support of the Foundation for Polish Science (FNP) through TEAM 2010-6/2 project co-financed by the EU European Regional Development Fund, and P.S. acknowledges the support of the Polish Ministry of Science and Higher Education (Grant No. N N202 055440).

APPENDIX A: THE FINAL FORMULAE

Below we give explicit expressions for the components of the mobility tensor for periodic systems with shear. From (17) the Hasimoto tensor takes the following form:

$$\mathbf{T}_{\mathrm{H}}(\mathbf{r}) = \sum_{\mathbf{n}} \left\{ \operatorname{erfc}\left(\frac{r_{\mathbf{n}}}{\sqrt{2\sigma^2}}\right) \mathbf{T}_0(\mathbf{r}_{\mathbf{n}}) + \frac{1}{4\sqrt{2\pi^3}\eta\sigma} \mathrm{e}^{-r_{\mathbf{n}}^2/2\sigma^2} \hat{\mathbf{r}}_{\mathbf{n}}\hat{\mathbf{r}}_{\mathbf{n}} \right\} - \frac{\sigma^2}{2\eta V}\mathbf{1} + \frac{1}{\eta V}{\sum_{\mathbf{n}}}' \left[\mathbf{1} - \hat{\mathbf{k}}_{\mathbf{n}}\hat{\mathbf{k}}_{\mathbf{n}} \left(1 + \frac{1}{2}\sigma^2 k_{\mathbf{n}}^2\right)\right] \frac{1}{k_{\mathbf{n}}^2} \mathrm{e}^{-k_{\mathbf{n}}^2\sigma^2/2} \cos(\mathbf{k}_{\mathbf{n}} \cdot \mathbf{r}). \tag{A1}$$

The mobility matrix components according to the definitions (32)–(37) take the form:

$$\begin{aligned}\mathbf{M}^{tt}(\mathbf{r}; a_i, a_j) = {} & \sum_{\mathbf{n}} \left\{ \mathbf{M}^{tt}_{np}(\mathbf{r}_{\mathbf{n}}; a_i, a_j) \operatorname{erfc}\left(\frac{r_{\mathbf{n}}}{\sqrt{2\sigma^2}}\right) \right. \\ & \left. + \left[\mathbf{1}\left(\frac{A_{ij}^2}{3\sigma^2} + \frac{2A_{ij}^2}{3r_{\mathbf{n}}^2}\right) + \hat{\mathbf{r}}_{\mathbf{n}}\hat{\mathbf{r}}_{\mathbf{n}}\left(\frac{A_{ij}^2 r_{\mathbf{n}}^2}{3\sigma^4} - \frac{2A_{ij}^2}{3\sigma^2} + 1 - \frac{2A_{ij}^2}{r_{\mathbf{n}}^2}\right)\right] \frac{1}{4\sqrt{2\pi^3}\eta\sigma} \mathrm{e}^{-r_{\mathbf{n}}^2/2\sigma^2} \right\} \\ & - \frac{\sigma^2}{2\eta V}\mathbf{1} + \frac{1}{\eta V}{\sum_{\mathbf{n}}}' \left[\mathbf{1} - \hat{\mathbf{k}}_{\mathbf{n}}\hat{\mathbf{k}}_{\mathbf{n}} \left(1 + \frac{1}{2}\sigma^2 k_{\mathbf{n}}^2\right)\right] \left(1 - \frac{A_{ij}^2}{3} k_{\mathbf{n}}^2\right) \frac{1}{k_{\mathbf{n}}^2} \mathrm{e}^{-k_{\mathbf{n}}^2\sigma^2/2} \cos(\mathbf{k}_{\mathbf{n}} \cdot \mathbf{r}),\end{aligned} \tag{A2}$$

$$\begin{aligned}\mathbf{M}^{tt}_S(a) = {} & \frac{1}{4\sqrt{2\pi^3}\sigma\eta}\left(-1 + \frac{a^2}{9\sigma^2}\right)\mathbf{1} \\ & + {\sum_{\mathbf{n}}}' \left\{ \mathbf{M}^{tt}_{np}(\mathbf{r}_{0\mathbf{n}}; a, a) \operatorname{erfc}\left(\frac{r_{0\mathbf{n}}}{\sqrt{2\sigma^2}}\right) \right. \\ & \left. + \left[\mathbf{1}\left(\frac{a^2}{3\sigma^2} + \frac{2a^2}{3r_{0\mathbf{n}}^2}\right) + \hat{\mathbf{r}}_{0\mathbf{n}}\hat{\mathbf{r}}_{0\mathbf{n}}\left(\frac{a^2 r_{0\mathbf{n}}^2}{3\sigma^4} - \frac{2a^2}{3\sigma^2} + 1 - \frac{2a^2}{r_{0\mathbf{n}}^2}\right)\right] \frac{1}{4\sqrt{2\pi^3}\eta\sigma} \mathrm{e}^{-r_{0\mathbf{n}}^2/2\sigma^2} \right\} \\ & - \frac{\sigma^2}{2\eta V}\mathbf{1} + \frac{1}{\eta V}{\sum_{\mathbf{n}}}' \left[\mathbf{1} - \hat{\mathbf{k}}_{\mathbf{n}}\hat{\mathbf{k}}_{\mathbf{n}} \left(1 + \frac{1}{2}\sigma^2 k_{\mathbf{n}}^2\right)\right] \left(1 - \frac{a^2}{3} k_{\mathbf{n}}^2\right) \frac{1}{k_{\mathbf{n}}^2} \mathrm{e}^{-k_{\mathbf{n}}^2\sigma^2/2},\end{aligned} \tag{A3}$$

$$\mathbf{M}^{rr}(\mathbf{r}) = \sum_{\mathbf{n}} \left\{ \mathbf{M}^{rr}_{np}(\mathbf{r}_n) \operatorname{erfc}\left(\frac{r_{\mathbf{n}}}{\sqrt{2\sigma^2}}\right) - \left[\mathbf{1}\left(\frac{1}{3\sigma^2} + \frac{2}{3r_{\mathbf{n}}^2}\right) + \hat{\mathbf{r}}_{\mathbf{n}}\hat{\mathbf{r}}_{\mathbf{n}}\left(\frac{r_{\mathbf{n}}^2}{3\sigma^4} - \frac{2}{3\sigma^2} - \frac{2}{r_{\mathbf{n}}^2}\right)\right] \frac{3}{16\sqrt{2\pi^3}\eta\sigma} \mathrm{e}^{-r_{\mathbf{n}}^2/2\sigma^2} \right\} + \frac{1}{4\eta V} \sum_{\mathbf{n}}{}' \left[\mathbf{1} - \hat{\mathbf{k}}_{\mathbf{n}}\hat{\mathbf{k}}_{\mathbf{n}}\left(1 + \frac{1}{2}\sigma^2 k_{\mathbf{n}}^2\right)\right] \mathrm{e}^{-k_{\mathbf{n}}^2\sigma^2/2} \cos(\mathbf{k}_{\mathbf{n}} \cdot \mathbf{r}), \tag{A4}$$

$$\mathbf{M}^{rr}_S = -\frac{1}{48\sqrt{2\pi^3}\sigma^3\eta}\mathbf{1} + \sum_{\mathbf{n}}{}' \left\{ \mathbf{M}^{rr}_{np}(\mathbf{r}_{0n}) \operatorname{erfc}\left(\frac{r_{0\mathbf{n}}}{\sqrt{2\sigma^2}}\right) - \left[\mathbf{1}\left(\frac{1}{3\sigma^2} + \frac{2}{3r_{0\mathbf{n}}^2}\right) + \hat{\mathbf{r}}_{0\mathbf{n}}\hat{\mathbf{r}}_{0\mathbf{n}}\left(\frac{r_{0\mathbf{n}}^2}{3\sigma^4} - \frac{2}{3\sigma^2} - \frac{2}{r_{0\mathbf{n}}^2}\right)\right] \frac{3}{16\sqrt{2\pi^3}\eta\sigma} \mathrm{e}^{-r_{0\mathbf{n}}^2/2\sigma^2} \right\} + \frac{1}{4\eta V} \sum_{\mathbf{n}}{}' \left[\mathbf{1} - \hat{\mathbf{k}}_{\mathbf{n}}\hat{\mathbf{k}}_{\mathbf{n}}\left(1 + \frac{1}{2}\sigma^2 k_{\mathbf{n}}^2\right)\right] \mathrm{e}^{-k_{\mathbf{n}}^2\sigma^2/2}, \tag{A5}$$

and

$$\mathbf{M}^{rt}(\mathbf{r}) = \sum_{\mathbf{n}} \left[\mathbf{M}^{rt}_{np}(\mathbf{r}_n) \operatorname{erfc}\left(\frac{r_{\mathbf{n}}}{\sqrt{2\sigma^2}}\right) + \boldsymbol{\epsilon} \cdot \hat{\mathbf{r}}_{\mathbf{n}} \frac{1}{r_{\mathbf{n}}} \frac{1}{4\sqrt{2\pi^3}\eta\sigma} \mathrm{e}^{-r_{\mathbf{n}}^2/2\sigma^2} \right] + \frac{1}{2\eta V} \sum_{\mathbf{n}}{}' \boldsymbol{\epsilon} \cdot \hat{\mathbf{k}}_{\mathbf{n}} \frac{1}{k_{\mathbf{n}}} \mathrm{e}^{-k_{\mathbf{n}}^2\sigma^2/2} \sin(\mathbf{k}_{\mathbf{n}} \cdot \mathbf{r}), \tag{A6}$$

$$\mathbf{M}^{rt}_S = 0, \tag{A7}$$

$$\mathbf{M}^{tr}(\mathbf{r}; a_{i,}, a_j) = \mathbf{M}^{rt}(\mathbf{r}; a_{j,}, a_i), \tag{A8}$$

$$\mathbf{M}^{td}(\mathbf{r}; a_i, a_j) = \sum_{\mathbf{n}} \mathbf{M}^{td}_{np}\left(\mathbf{r}_n; a_i, a_j\right) \operatorname{erfc}\left(\frac{r_{\mathbf{n}}}{\sqrt{2\sigma^2}}\right) + \frac{5a_j^3}{3\sqrt{2\pi}\sigma} \sum_{\mathbf{n}} \mathrm{e}^{-r_{\mathbf{n}}^2/2\sigma^2} \left\{ -\frac{16}{15}\mathscr{A}_{ij}^2 \left(\frac{1}{\sigma^2 r_{\mathbf{n}}} + \frac{3}{r_{\mathbf{n}}^3}\right) \mathbf{1}\hat{\mathbf{r}}_{\mathbf{n}} + \left[-\frac{4\mathscr{A}_{ij}^2 r_{\mathbf{n}}^3}{15\sigma^6} + \left(-\frac{1}{\sigma^2} + \frac{8\mathscr{A}_{ij}^2}{15\sigma^4}\right) r_{\mathbf{n}} + \left(-3 + \frac{8\mathscr{A}_{ij}^2}{3\sigma^2}\right) \frac{1}{r_{\mathbf{n}}} + 8\frac{\mathscr{A}_{ij}^2}{r_{\mathbf{n}}^3} \right] \hat{\mathbf{r}}_{\mathbf{n}}\hat{\mathbf{r}}_{\mathbf{n}}\hat{\mathbf{r}}_{\mathbf{n}} \right\} - \frac{20\pi a_j^3}{3V} \sum_{\mathbf{n}}{}' \left[\mathbf{1} - \hat{\mathbf{k}}_{\mathbf{n}}\hat{\mathbf{k}}_{\mathbf{n}}\left(1 + \frac{1}{2}\sigma^2 k_{\mathbf{n}}^2\right)\right] \hat{\mathbf{k}}_{\mathbf{n}} \frac{15 - 4\mathscr{A}_{ij}^2 k_{\mathbf{n}}^2}{15k_{\mathbf{n}}} \mathrm{e}^{-k_{\mathbf{n}}^2\sigma^2/2} \sin(\mathbf{k}_{\mathbf{n}} \cdot \mathbf{r}), \tag{A9}$$

$$\mathbf{M}^{td}_S(a) = 0, \tag{A10}$$

$$\mathbf{M}^{rd}\left(\mathbf{r}, a_j\right) = \sum_{\mathbf{n}} \left\{ \mathbf{M}^{rd}_{np}(\mathbf{r}_n; a_j) \operatorname{erfc}\left(\frac{r_{\mathbf{n}}}{\sqrt{2\sigma^2}}\right) - \left(\boldsymbol{\epsilon} \cdot \hat{\mathbf{r}}_{\mathbf{n}}\right) \hat{\mathbf{r}}_{\mathbf{n}} \frac{5a_j^3}{3\sqrt{2\pi}\sigma} \mathrm{e}^{-r_{\mathbf{n}}^2/2\sigma^2} \left(\frac{1}{\sigma^2} + \frac{3}{r_{\mathbf{n}}^2}\right) \right\} + \frac{10\pi a_j^3}{3V} \sum_{\mathbf{n}}{}' \left(\boldsymbol{\epsilon} \cdot \hat{\mathbf{k}}_{\mathbf{n}}\right) \hat{\mathbf{k}}_{\mathbf{n}} \mathrm{e}^{-k_{\mathbf{n}}^2\sigma^2/2} \cos(\mathbf{k}_{\mathbf{n}} \cdot \mathbf{r}), \tag{A11}$$

$$\mathbf{M}^{rd}_S(a) = \sum_{\mathbf{n}}{}' \left\{ \mathbf{M}^{rd}_{np}(\mathbf{r}_{0\mathbf{n}}; a) \operatorname{erfc}\left(\frac{r_{0\mathbf{n}}}{\sqrt{2\sigma^2}}\right) - \left(\boldsymbol{\epsilon} \cdot \hat{\mathbf{r}}_{0\mathbf{n}}\right) \hat{\mathbf{r}}_{0\mathbf{n}} \frac{5a}{3\sqrt{2\pi}\sigma} \mathrm{e}^{-r_{0\mathbf{n}}^2/2\sigma^2} \left(\frac{a^2}{\sigma^2} + \frac{3a^2}{r_{0\mathbf{n}}^2}\right) \right\} + \frac{10\pi a^3}{3V} \sum_{\mathbf{n}}{}' \left(\boldsymbol{\epsilon} \cdot \hat{\mathbf{k}}_{\mathbf{n}}\right) \hat{\mathbf{k}}_{\mathbf{n}} \mathrm{e}^{-k_{\mathbf{n}}^2\sigma^2/2}, \tag{A12}$$

where the primes at the summation symbol indicate that the terms $\mathbf{n} = 0$ are to be omitted,

$$\mathbf{r}_{0\mathbf{n}} = \mathbf{L} \cdot \mathbf{n}, \tag{A13}$$

$[\boldsymbol{\epsilon} \cdot \hat{\mathbf{r}}]_{\alpha\beta} = \epsilon_{\alpha\beta\gamma} [\hat{\mathbf{r}}]_\gamma$, $[\mathbf{1}\hat{\mathbf{r}}]_{\alpha\beta\gamma} = \delta_{\alpha\beta} [\hat{\mathbf{r}}]_\gamma$, and the Greek indices $\alpha, \beta = 1, 2, 3$ correspond to the Cartesian components. The non-periodic mobility components are

$$\mathbf{M}^{tt}_{np}(\mathbf{r}; a_i, a_j) = \frac{1}{8\pi\eta r}\left[\left(1 + \frac{2A^2_{ij}}{3r^2}\right)\mathbf{1} + \left(1 - \frac{2A^2_{ij}}{r^2}\right)\hat{\mathbf{r}}\hat{\mathbf{r}}\right], \tag{A14}$$

$$\mathbf{M}^{rr}_{np}(\mathbf{r}) = -\frac{1}{16\pi\eta r^3}\left(\mathbf{1} - 3\hat{\mathbf{r}}\hat{\mathbf{r}}\right), \tag{A15}$$

$$\mathbf{M}^{rt}_{np}(\mathbf{r}) = \frac{1}{8\pi\eta r^2}\boldsymbol{\epsilon} \cdot \hat{\mathbf{r}}, \tag{A16}$$

$$\mathbf{M}^{td}_{np}(\mathbf{r}; a_i, a_j) = \frac{5a_j^3}{6}\left[-\frac{16}{5}\frac{\mathscr{A}^2_{ij}}{r^4}\mathbf{1}\hat{\mathbf{r}} + \left(-3\frac{1}{r^2} + 8\frac{\mathscr{A}^2_{ij}}{r^4}\right)\hat{\mathbf{r}}\hat{\mathbf{r}}\hat{\mathbf{r}}\right], \tag{A17}$$

$$\mathbf{M}^{rd}_{np}(\mathbf{r}; a_j) = -\frac{5a_j^3}{2r^3}(\boldsymbol{\epsilon} \cdot \hat{\mathbf{r}})\,\hat{\mathbf{r}}. \tag{A18}$$

The regularizing corrections for mobility, which are non-zero only if the particles overlap, i.e., for $r_{\mathbf{n}} \le 2a$, can be found in Appendix B.

APPENDIX B: THE REGULARIZING CORRECTIONS

Here we give the explicit expressions for the full correction matrix $\mathbf{Y}$ as defined in (32)–(37). In Ref. 25 it has been shown that the same corrections as those derived for the infinite space can also be used for other boundary conditions, including the periodic systems. The formulae for the hydrodynamic matrices for different-sized spheres, derived in Ref. 26, lead to the following expressions for the correction matrix:

$$\begin{aligned}\mathbf{Y}^{tt}(\mathbf{r}; a_i, a_j) = \Theta((a_i + a_j) - r)\Bigg\{ &\\ &+ \Theta(r - (a_> - a_<))\frac{1}{6\pi\eta a_i a_j}\left[\frac{16r^3(a_i + a_j) - ((a_i - a_j)^2 + 3r^2)^2}{32r^3}\mathbf{1} + \frac{3((a_i - a_j)^2 - r^2)^2}{32r^3}\hat{\mathbf{r}}\hat{\mathbf{r}}\right]\\ &+ \Theta((a_> - a_<) - r)\frac{1}{6\pi\eta a_>} - \mathbf{M}^{tt}_{np}(\mathbf{r}; a_i, a_j)\Bigg\},\end{aligned} \tag{B1}$$

$$\begin{aligned}\mathbf{Y}^{rr}(\mathbf{r}; a_i, a_j) = \Theta((a_i + a_j) - r)\Bigg\{ &\\ &+ \Theta(r - (a_> - a_<))\frac{1}{8\pi\eta a_i^3 a_j^3}\left[\mathcal{F}(\mathbf{r}; a_i, a_j)\mathbf{1} + \mathcal{G}(\mathbf{r}; a_i, a_j)\hat{\mathbf{r}}\hat{\mathbf{r}}\right]\\ &+ \Theta((a_> - a_<) - r)\frac{1}{8\pi\eta a_>^3}\mathbf{1} - \mathbf{M}^{rr}_{np}(\mathbf{r})\Bigg\},\end{aligned} \tag{B2}$$

$$\begin{aligned}\mathbf{Y}^{rt}(\mathbf{r}; a_i, a_j) = \Theta((a_i + a_j) - r)\Bigg\{ &\\ &+ \Theta(r - (a_> - a_<))\frac{1}{16\pi\eta a_i^3 a_j}\left[\frac{(a_i - a_j + r)^2\left(a_j^2 + 2a_j(a_i + r) - 3(a_i - r)^2\right)}{8r^2}\right]\boldsymbol{\epsilon} \cdot \hat{\mathbf{r}}\\ &+ \Theta((a_> - a_<) - r)\theta(a_i - a_j)\frac{r}{\zeta^{rr}_i}\boldsymbol{\epsilon} \cdot \hat{\mathbf{r}} - \mathbf{M}^{rt}_{np}(\mathbf{r})\Bigg\},\end{aligned} \tag{B3}$$

$$\mathbf{Y}^{tr}(\mathbf{r}; a_i, a_j) = \mathbf{Y}^{rt}(\mathbf{r}; a_j, a_i), \tag{B4}$$

$$\begin{aligned}\mathbf{Y}^{td}(\mathbf{r}; a_i, a_j) = \Theta((a_i + a_j) - r)\Bigg\{ &\\ &+ \Theta(r - (a_> - a_<))\frac{5}{6}a_j\left[\mathcal{H}(\mathbf{r}; a_i, a_j)\mathbf{1}\hat{\mathbf{r}} + \mathcal{J}(\mathbf{r}; a_i, a_j)\hat{\mathbf{r}}\hat{\mathbf{r}}\hat{\mathbf{r}}\right]\\ &- \Theta((a_> - a_<) - r)\theta(a_j - a_i)r\mathbf{1}\hat{\mathbf{r}} - \mathbf{M}^{td}_{np}(\mathbf{r}; a_i, a_j)\Bigg\},\end{aligned} \tag{B5}$$

$$\mathbf{Y}^{rd}(\mathbf{r};a_i,a_j)=\Theta((a_i+a_j)-r)\Big\{ \\ -\Theta(r-(a_>-a_<))\frac{5}{3a_i^3}\mathcal{G}(\mathbf{r};a_i,a_j)\,(\epsilon\cdot\hat{\mathbf{r}})\,\hat{\mathbf{r}}-\mathbf{M}^{rd}_{np}(\mathbf{r};a_j)\Big\}, \tag{B6}$$

where

$$\mathcal{F}(\mathbf{r};a_i,a_j)=\frac{5r^6-54r^4A_{ij}^2+32r^3\left(a_i^3+a_j^3\right)-9r^2\left(a_i^2-a_j^2\right)^2-(a_i-a_j)^4\left(a_i^2+4a_ia_j+a_j^2\right)}{64r^3}, \tag{B7a}$$

$$\mathcal{G}(\mathbf{r};a_i,a_j)=\frac{3[(a_i-a_j)^2-r^2]^2\left(a_i^2+4a_ia_j+a_j^2-r^2\right)}{64r^3}, \tag{B7b}$$

$$\mathcal{H}(\mathbf{r};a_i,a_j)=\frac{10r^6-24a_ir^5+15r^4\left(a_i^2-a_j^2\right)-(a_i-a_j)^5(a_i+5a_j)}{40a_ia_jr^4}, \tag{B7c}$$

$$\mathcal{J}(\mathbf{r};a_i,a_j)=\frac{[(a_i-a_j)^2-r^2]^2[r^2-(a_i-a_j)(a_i+5a_j)]}{16a_ia_jr^4}, \tag{B7d}$$

$[\epsilon\cdot\hat{\mathbf{r}}]_{\alpha\beta}=\epsilon_{\alpha\beta\gamma}\,[\hat{\mathbf{r}}]_\gamma$, $[\mathbf{1}\hat{\mathbf{r}}]_{\alpha\beta\gamma}=\delta_{\alpha\beta}\,[\hat{\mathbf{r}}]_\gamma$, $a_>$ ($a_<$) denotes the radius of a larger (smaller) particle in the pair i and j and $\Theta(x)$ is the Heaviside function. With so defined corrections the mobility matrix (the translational-rotational part) is always positive definite, as demonstrated by Ref. 25, thus allowing for simulations of the Brownian dynamics of suspensions.

[1] J. F. Brady and J. F. Morris, J. Fluid Mech. **348**, 103 (1997).
[2] J. Bergenholtz, J. Brady, and M. Vicic, J. Fluid Mech. **456**, 239 (2002).
[3] J. Vermant and M. J. Solomon, J. Phys.: Condens. Matter **17**, R187 (2005).
[4] E. S. G. Shaqfeh, J. Non-Newton. Fluid. **130**, 1 (2005).
[5] P. Szymczak and M. Cieplak, J. Phys.: Condens. Matter **23**, 033102 (2011).
[6] D. E. Dunstan, P. Hamilton-Brown, P. Asimakis, W. Ducker, and J. Bertolini, Protein Eng. Des. Sel. **22**, 741 (2009).
[7] A. Loksztejn and W. Dzwolak, J. Mol. Biol. **395**, 643 (2010).
[8] O. B. Usta, J. E. Butler, and A. J. Ladd, Phys. Fluids **18**, 031703 (2006).
[9] A. Onuki, J. Phys.: Condens. Matter **9**, 6119 (1997).
[10] P. D. Olmsted, Curr. Opin. Colloid Interface Sci. **4**, 95 (1999).
[11] J. K. G. Dhont, *An Introduction to Dynamics of Colloids* (Elsevier Science, 1996).
[12] H. Tanaka, J. Phys.: Condens. Matter **13**, 4637 (2001).
[13] P. Wojtaszczyk and J. B. Avalos, Phys. Rev. Lett. **80**, 754 (1998).
[14] R. G. Larson and J. J. Magda, Macromolecules **22**, 3004 (1989).
[15] P. Szymczak and M. Cieplak, J. Phys.: Condens. Matter **19**, 285224 (2007).
[16] T. Frembgen-Kesner and A. H. Elcock, J. Chem. Theory Comput. **5**, 242 (2009).
[17] T. Ando and J. Skolnick, Biophys. J. **104**, 96 (2013).
[18] A. Lees and S. Edwards, J. Phys. C **5**, 1921 (1972).
[19] D. J. Evans and G. Morriss, *Statistical Mechanics of Nonequilibrium Liquids* (Cambridge University Press, 2008).
[20] H. Kobayashi and R. Yamamoto, J. Chem. Phys. **134**, 064110 (2011).
[21] A. J. Wagner and I. Pagonabarraga, J. Stat. Phys. **107**, 521 (2002).
[22] N. Kikuchi, C. Pooley, J. Ryder, and J. Yeomans, J. Chem. Phys. **119**, 6388 (2003).
[23] S. Kim and S. J. Karrila, *Microhydrodynamics: Principles and Selected Applications* (Butterworth-Heinemann, London, 1991).
[24] G. Nägele, *Computational Condensed Matter Physics*, Matter and Materials Vol. 32, edited by S. Blügel, G. Gompper, E. Koch, H. Müller-Krumbhaar, R. Spatschek, and R. G. Winkler (Forschungszentrum Jülich, 2006).
[25] E. Wajnryb, K. A. Mizerski, P. J. Zuk, and P. Szymczak, J. Fluid Mech. **731**, R3 (2013).
[26] P. J. Zuk, E. Wajnryb, K. A. Mizerski, and P. Szymczak, J. Fluid Mech. **741**, R5 (2014).
[27] H. Hasimoto, J. Fluid Mech. **5**, 317 (1959).
[28] D. L. Ermak and J. A. McCammon, J. Chem. Phys. **69**, 1352 (1978).
[29] E. Wajnryb, P. Szymczak, and B. Cichocki, Physica A **335**, 339 (2004).
[30] B. Cichocki and B. Felderhof, Physica A **159**, 19 (1989).
[31] A. Zygmund, *Trigonometric Series* (Cambridge University Press, 1988), Vol. 1.
[32] C. W. J. Beenakker, J. Chem. Phys. **85**, 1581 (1986).
[33] A. Jain, P. Sunthar, B. Dünweg, and J. R. Prakash, Phys. Rev. E **85**, 066703 (2012).
[34] C. Stoltz, J. J. Pablo, and M. D. Graham, J. Rheol. **50**, 137 (2006).
[35] J. F. Brady, R. J. Phillips, J. C. Lester, and G. Bossis, J. Fluid Mech. **195**, 257 (1988).
[36] T. Zhou and S. B. Chen, J. Chem. Phys. **124**, 034904 (2006).
[37] B. Felderhof and R. Jones, J. Math. Phys. **30**, 339 (1989).